**Electronic Supplementary Material**

# Clinical Translation of Tumor Acidosis Measurements with AcidoCEST MRI

**Journal: Molecular Imaging and Biology**

Kyle M. Jones, B.S.,[1] Edward A. Randtke, Ph.D.,[2] Eriko Yoshimaru, Ph.D.,[3] Christine M. Howison, B.S.,[2] Pavani Chalasani, M.D.,[4] Robert R. Klein, M.D.,[5] Setsuko K. Chambers, M.D.,[3,6] Philip H. Kuo, M.D., Ph.D.,[1,2,3] and Mark D. Pagel, Ph.D.[1,2,3]

1. Biomedical Engineering Graduate Interdisciplinary Program, University of Arizona, Tucson, AZ
2. Department of Medical Imaging, University of Arizona, Tucson, AZ
3. University of Arizona Cancer Center, Tucson, AZ
4. Division of Hematology-Oncology, University of Arizona, Tucson, AZ
5. Department of Pathology, University of Arizona, Tucson, AZ
6. Department of Obstetrics and Gynecology, University of Arizona, Tucson, AZ

Corresponding Author:
Mark D. Pagel, Ph.D.
Department of Medical Imaging
University of Arizona
1515 N. Campbell Ave.
Tucson, AZ 85724-5024
Tel: (520)-404-7049
Email: mpagel@u.arizona.edu

**Studies of chemical solutions**

To perform studies with a 600 MHZ NMR spectrometer, solutions of 78 mM iopamidol were adjusted to pH values of 5.82, 6.08, 6.47, 6.72, 6.93, 7.42 and 7.67. A solution of 39 mM of the agent was prepared at pH 6.72 to ensure that the estimated exchange rate ($k_{ex}$) of each exchanging pool of iopamidol was independent of concentration.

To perform studies with a 7 T MRI scanner, solutions of 10 mM iopamidol were adjusted to pH values of 5.36, 6.40, 6.60, 6.78, 6.96, 7.13, 7.33, and 7.54. Each solution was placed in a 300 µl centrifuge tube and all samples were placed in a box filled with agar. The box was placed in a 7T Biospec MRI scanner (Bruker Biospin, Billerica, MA) maintained at 37.0 $\pm$ 0.5 °C using warm air (SA Instruments, Inc., Stony Brook, NY). To maintain the temperature of the box, a fiber optic sensor was inserted into the agar, which controlled the warm air based on the temperature of the agar. Four acidoCEST MRI scans were acquired using a CEST-FISP MRI protocol with parameters listed in Table S1. Saturation frequencies were iterated from -10 ppm to 10 ppm in increments of 0.2 ppm.

To perform studies with a 7 T MRI scanner, solutions of 50 mM iopamidol were adjusted to pH values of 5.21, 6.42, 6.63, 6.76, 7.03, and 7.22. Each solution was placed in a 50 ml conical tube and all samples were placed in a Styrofoam container that was filled with water. The container was wrapped with a heating pad to maintain a 37.0 $\pm$ 0.5 °C temperature, and placed in a 3T MRI scanner. A fiber optic sensor was inserted into the water inside the container, which controlled the heating pad. Four acidoCEST MRI scans were acquired using a CEST-FISP MRI protocol with parameters listed in Table S1. Saturation frequencies were iterated from -10 ppm to 10 ppm in increments of 0.2 ppm.

## MRI acquisition parameters

The MRI acquisition parameters for imaging chemical solutions, mouse models, and patients, are listed in table S1. The CEST-FISP MRI protocol is described in reference 1.

Table S1. Summary of imaging parameters

| | 7 T chemical solutions and flank tumor model | 3 T chemical solutions and patients | |
|---|---|---|---|
| | | Ovarian | Ductal Carcinoma |
| **Anatomical MRI** | | | |
| Acq Sequence | Spin Echo | Gradient Echo | Spin Echo |
| TR | 1076 msec | 4.36 msec | 2.96 msec |
| TE | 12.7 msec | 2.3 msec | 1.2 msec |
| Slice thickness | 1 mm | 3 mm | 1 mm |
| Number of slices | 10 | 88 | 60 |
| Orientation | Axial | Axial | Axial |
| In-plane resolution | 453x453 $\mu m^2$ | 1.5x1.5 $mm^2$ | 1.4x1.4 $mm^2$ |
| Matrix size | 128x128 | 288x216 | 288x248 |
| Field of view | 5.8x5.8 $cm^2$ | 42.0 $cm^2$ | 34.0 $cm^2$ |
| Number of averages | 1 | 1 | 1 |
| Respiration gating | No | No | No |
| Total acq. time | 2:17 min | 11 sec | 30 sec |
| **CEST-FISP MRI** | | | |
| $B_0$ correction | aciodCEST | WASSR | acidoCEST |
| TR | 3.70 msec | 4.47 msec | 4.47 msec |
| TE | 1.60 msec | 1.62 msec | 1.62 msec |
| Excitation Angle | $10^o$ | $15^o$ | $15^o$ |
| Slice thickness | 1 mm | 10 mm | 10 mm |
| Number of slices | 1 | 1 | 1 |
| Orientation | Axial | Axial | Axial |
| In-plane resolution | 453x453 $\mu m^2$ | 2x2 $mm^2$ | 2x2 $mm^2$ |
| Matrix size | 128x128 | 160x160 | 160x160 |
| Field of view | 5.8x5.8 $cm^2$ | 32.0 $cm^2$ | 32.0 $cm^2$ |
| Number of averages | 1 | 1 | 1 |
| Respiration gating | No | No | No |
| Sat. Power | 3.5 $\mu T$ | 1.5 $\mu T$ | 1.5 $\mu T$ |
| Sat. Pulse Shape | Half Gauss | Rectangular | Rectangular |
| Sat.Time | 5 sec | 1.0 sec | 2.0 sec |
| Acq. time (1 image) | 5.4 sec | 1.715 sec | 2.715 sec |
| Acq. time (Full CEST spectra) | 3:47 min | 36.0 sec | 57.0 sec |

**Preparation of the Mouse Model**

The University of Arizona Institutional Animal Care and Use Committee approved our studies with mouse models of human ovarian cancer. A flank tumor model was prepared by injecting $10^6$ epithelial SKOV3 tumor cells in 0.5 mL of 50% Matrigel™ in the subcutaneous rear flank of 10 female C.B-17/ICRACC white SCID mice at 4-8 weeks of age. Starting two weeks after cell injection, each mouse was evaluated with acidoCEST MRI each week for four weeks.

At the start of each MRI scan, 1.5-2.5% isoflurane in $O_2$ gas was used to anesthetize a mouse. The mouse was positioned in a customized cradle, and a pneumatic pad was positioned under the mouse to monitor respiration (SA Instruments, Inc., Stony Brook, NY). A fiber optic sensor was used to monitor core body temperature, which was maintained at $37.0 \pm 0.5^{o}C$ using warmed air. A tail vein was catheterized to deliver the contrast agent.

Table S2. Summary of mouse survival and agent uptake in tumor models

| Week | Flank Tumor Model | |
|---|---|---|
| | Number of mice imaged | Number of mice with sufficient contrast agent uptake |
| 1 | 10 | 4 |
| 2 | 10 | 3 |
| 3 | 10 | 4 |
| 4 | 10 | 5 |

**Bloch fitting and Lorentzian line shape fitting**

For Bloch and Lorentzian line shape fitting (a.k.a. Lorentzian fitting), a step size of $10^{-8}$ and a function tolerance of $10^{-8}$ was used. Initial values for Bloch fitting were pHe = 7.0; concentration = 10 mM; $T_1$ = 2.0 sec; $T_2$ = 0.056 sec; $B_0$ offset = 360 Hz (where $B_0$ offset is the water saturation shift offset for an individual pixel relative to the Larmor frequency); and two scale factors set to a value of 1 to account for the change in baseline between the pre-injection and post-injection scans. Initial values for Lorentzian fitting were widths of 2 ppm and amplitudes of 10% for both the 4.2 and 5.5 ppm peaks of iopamidol. The offsets of 4.2 and 5.5 ppm were also used as initial guesses for the location of the two peaks in the difference CEST spectrum. A line shape for the hydroxyl groups of iopamidol was not fit from *in vivo* studies due to their proximity to water. The $B_0$ offset was estimated by taking the minimum value in the CEST spectrum for both the pre and post injection images as the true water saturation offset frequency and adjusting all other saturation offset frequencies according to the $B_0$ offset estimate [2].

The Bloch equations are written as suggested by Murase [3]:

$$A = \begin{bmatrix} -\frac{1}{T_{2w}} - \chi k_{ex} & -(\omega_w - \omega) & 0 & k_{ex} & 0 & 0 & 0 \\ (\omega_w - \omega) & -\frac{1}{T_{2w}} - \chi k_{ex} & -\omega_{B1} & 0 & k_{ex} & 0 & 0 \\ 0 & \omega_{B1} & -\frac{1}{T_{1w}} - \chi k_{ex} & 0 & 0 & k_{ex} & \frac{M_w}{T_{1w}} \\ \chi k_{ex} & 0 & 0 & -\frac{1}{T_{2b}} - k_{ex} & -(\omega_b - \omega) & 0 & 0 \\ 0 & \chi k_{ex} & 0 & (\omega_b - \omega) & -\frac{1}{T_{2b}} - k_{ex} & -\omega_{B1} & 0 \\ 0 & 0 & \chi k_{ex} & 0 & \omega_{B1} & -\frac{1}{T_{1b}} - k_{ex} & \frac{\chi M_w}{T_{1b}} \\ 0 & 0 & 0 & 0 & 0 & 0 & 1 \end{bmatrix} \quad [A1]$$

where $T_{1w}$ = longitudinal relaxation time of water, $T_{2w}$ = transverse relaxation time of water, $T_{1b}$ = longitudinal relaxation time of iopamidol, $T_{2b}$ = transverse relaxation time of iopamidol, $\chi$ = mole

fraction of labile pool, $k_{ex}$ = exchange rate, $\omega_a$ = resonant frequency of water (rad/sec), $\omega_b$ = resonant frequency of labile pool (rad/sec), $\omega$ = RF irradiation frequency, and $\omega_{B1}$ = nutation rate (rad/sec).

This formula is fit in the same way as previously described by Woessner [4] except pH is fit directly instead of fitting $k_{ex}$. The exchange rate is related to pH (Eq. [A2]).

$$k_{ex} = k_0 + k_b \cdot 10^{Kw-pH} \qquad [A2]$$

where $k_w$ = water ionization constant, $k_0$ = uncatalyzed exchange rate, and $k_b$ = base catalyzed exchange rate.

The exchange rate of water and the 4 labile pools of iopamidol are determined, so the size of the matrix A is 16x16. To simulate the difference spectrum, data is simulated with $\chi$ = 0 and simulated with $\chi$ = estimated mole fraction. The difference of these spectra is compared to the experimental difference, and is fit via non-linear least squares.

The pH, $T_1$, $T_2$, agent concentration, $B_0$, and two scale factors to account for a shift in baseline are estimated from the fitting process. From our experience, pH primarily changes the shape of the CEST spectrum while the concentration, $T_1$, and the two scale factors primarily change the amplitude of the CEST spectrum. Therefore, the estimate of pH is largely independent of the other parameters being fit.

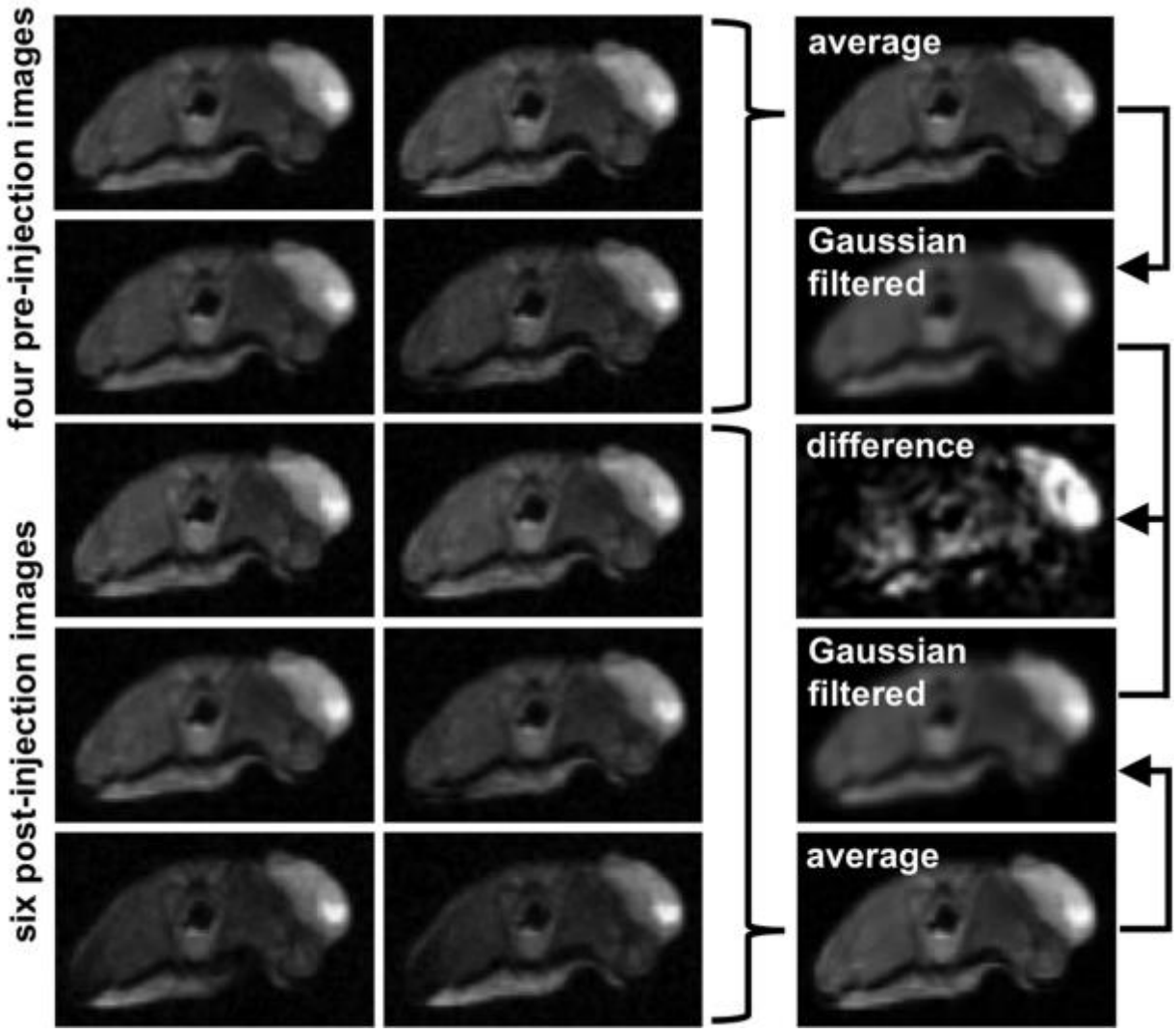


FIGURE S1. AcidoCEST MR image processing. The four pre-injection images were averaged to create an average pre-scan image, and the six post-injection images were averaged to create an average post-scan image. A Gaussian spatial filter was applied to both the average pre-scan and average post-scan images. The average, smoothed post-injection image was subtracted from the average, smoothed pre-injection image to create a difference image.

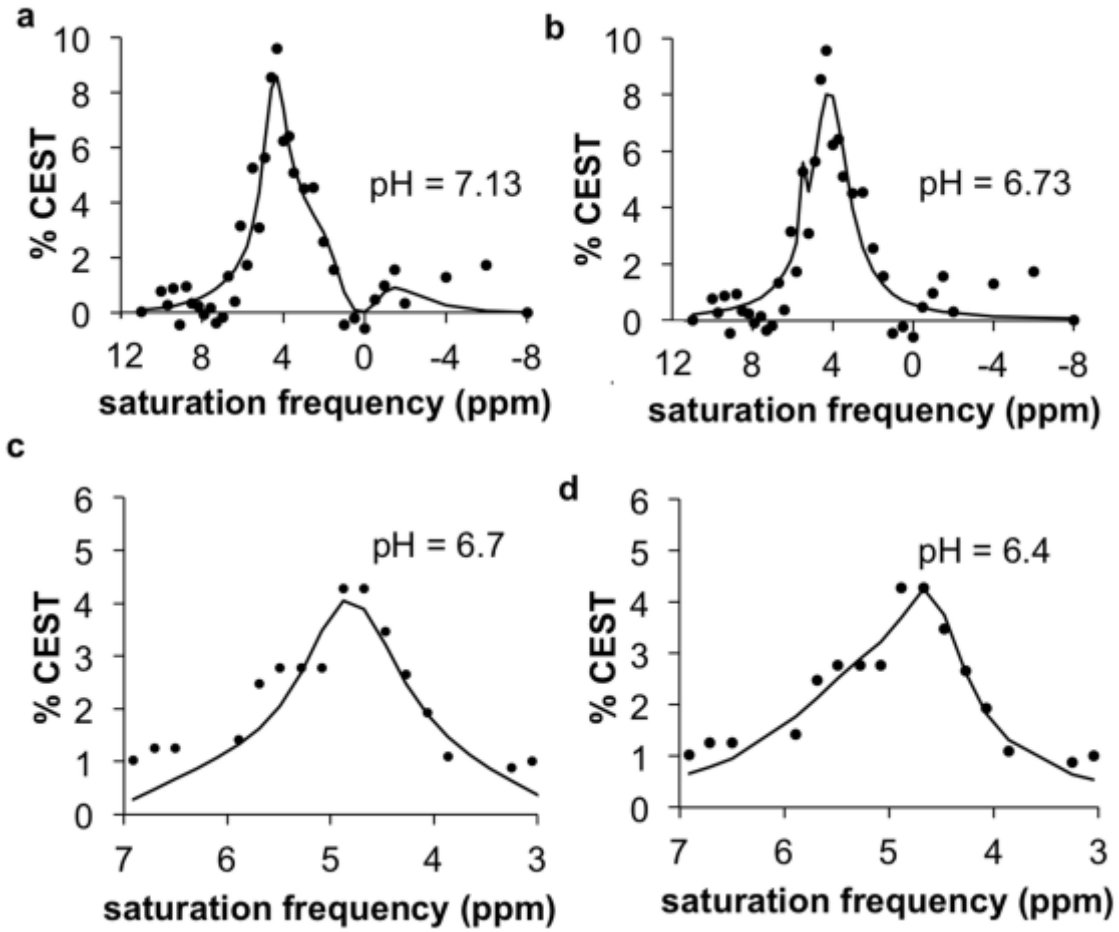


Fig. S2. Analyses of acidoCEST MRI results of the tumor models. A representative CEST spectrum from a pixel of the flank tumor model was analyzed by **a** Bloch fitting and **b** Lorentzian line shape fitting. A representative CEST spectrum from a pixel of the patient with metastatic ovarian cancer was analyzed with **c** Bloch fitting and **d** Lorentzian line shape fitting.

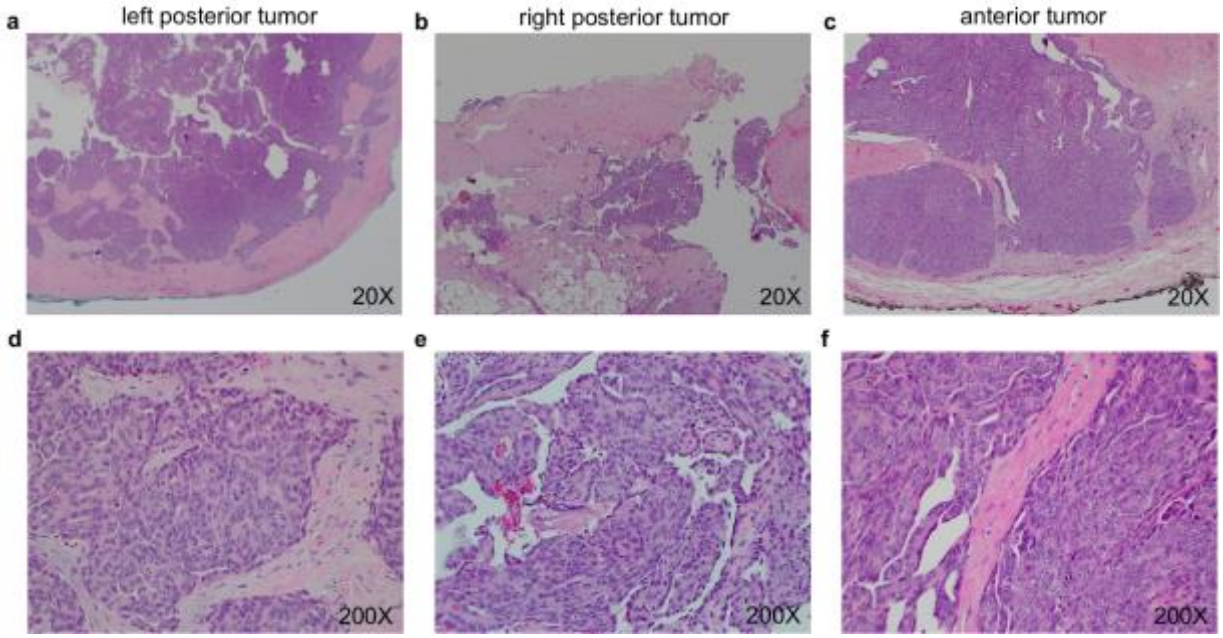


Figure S3. Histopathology of the metastatic ovarian tumors. Staining for collagen in **a,d)** the left posterior tumor, **b,e)** the right posterior tumor and **c,f)** anterior tumor showed higher fibrosity in the right posterior tumor and the rim of the left posterior tumor.

**References:**

1) Shah T, Lu L, Dell KM, Pagel MD, Griswold MA, Flask CA (2011) CEST-FISP: a novel technique for rapid chemical exchange saturation transfer MRI at 7T. Magn Reson Med 65:432-437.

2) Chen LQ, Randtke EA, Jones KM, et al. (2015) Evaluations of tumor acidosis within in vivo tumor models using parametric maps generated with acidoCEST MRI Mol Imaging Biol 17:488-496

3) Murase K, Tanki N. Numerical solutions to the time-dependent Bloch equations revisited. Magn Reson Imaging 2011;1:126-131.

4) Woessner DE, Zhang S, Merritt ME, Sherry AD. Numerical solution of the Bloch equations provides insights into the optimum design of PARACEST agents for MRI. Magn Reson Med 2005;4:790-799.